MAGNETOSTRICTIVE CURRENT SENSOR DEVELOPMENT
USING FIBER OPTICS

Stephen E. Williams
University Undergraduate Fellow, 1990-91
Texas A&M University
Department of Electrical Engineering

APPROVED:

Fellows Advisor Mark H. Weichold

Honors Program Director J. I. Kinchen

MAGNETOSTRICTIVE CURRENT SENSOR DEVELOPMENT USING FIBER OPTICS

Stephen E. Williams
Texas A&M University

Abstract—The ability to develop a fiber optic current sensor utilizing the magnetostrictive characteristics of nickel (Ni) has been proven. A Mach-Zehnder interferometer, which had a 2.5-μm layer of Ni 15-cm long on its sensing arm, was found to accurately detect magnetic fields as small as 40 gauss. Ni was deposited via DC sputter directly onto the SiO_2 buffer of the 1.3-μm single mode fiber. There is sufficient evidence that a two-step process involving the electron-beam deposition of 274 Å of chromium (Cr), 226 Å of Ni, and a Ni electroplate of greater than 10-μm thickness can be achieved. Such a deposition should yield a 16-fold increase in sensor sensitivity.

Introduction

Due to their small size, optical fibers are the subject of much interest for sensor applications. With regard to electrical power systems, fiber optic current sensors are beginning to provide an alternative to the elaborate transformer/transducer sensor systems presently in use. Current transformers, while being accurate, are very large, costly, and occasionally suffer explosive failures. Optical sensors offer a safer, smaller alternative.

Research on fiber optic current sensors has primarily involved studying the Faraday effect in optical fibers and in magnetooptic materials such as the rare-earth iron garnets. The Faraday effect is known as the ability of a magnetic field to modulate the polarization of electromagnetic radiation within a material. If a linearly polarized beam of light is incident on a magneto-optic material placed in the presence of a magnetic field oriented along the light's path, the light will exit the substance with an angle of polarization rotated relative to the incident beam. Since this rotation is directly related to field intensity via a material-dependent Verdet constant, current measurements are possible.

Another optical current sensing system, which has not been significantly explored, is based on the phenomenon of magnetostriction. As the name implies, magnetostriction is an induced change in the dimensions of a material due to an applied magnetic field. While magnetostriction is not an optical effect, we have found a method by which fiber optics and magnetostriction can be merged to yield a miniature magnetic field sensor.

The relatively simple sensor consists of a laser light source, an interferometer, a photodetector appropriate for use with the laser, and some signal analysis circuitry. Typically the photodetector could be an avalanche photodiode (APD), a universal photodetector (UDT), or a simple photodiode. For output signal analysis, the detector should be connected to a lock-in amplifier referenced at the appropriate frequency. The output of the lock-in amplifier could then be more easily analyzed by application-specific hardware and software such as an analog-to-digital (A/D) converter connected to a microprocessor or microcontroller running data acquisition or control programs.

The transducer element of the sensor system is the interferometer, which can convert information about the magnetic field into optical data through the use of an appropriately configured sensing arm. While the type of interferometer is not critical for describing an abstract system, the two-arm Mach-Zehnder(M-Z) configuration was deemed more useful as a development tool since it is more easily constructed and less dependent on a stable source than the Fabry-Perot(F-P) interferometer. The F-P interferometer is being used by other researchers at Texas A&M who are developing highly sensitive temperature and strain transducers [1]. Following further characterization of the M-Z current sensor, the next stage of development would be to obtain similar results with an F-P current sensor, as the one-armed F-P is more suitable for *in situ* sensing applications.

The transducer attached to the interferometer sensing arm for

magnetic field detection was a 2.5μm layer of nickel (Ni). A thicker layer of nickel would have been desirable, but it was not readily obtained due to process limitations.

Objectives

While it is apparent that the ultimate goal of such research would be the production of a working current sensor, the period of study should first entail a review of published papers concerning fiber optics and magneto-optic materials. The review should then lead to the determination of a group of materials and sensor configurations which could undergo laboratory testing. The second phase of research would involve developing a sensor system capable of making rudimentary current or magnetic field measurements, if possible. Since research time is presently limited to one academic year with a Spring, 1991, completion date, the final objective of this project is to prove that the concept of the fiber optic current sensor is valid, rather than produce a complete working sensor system.

Part One — Preliminary Research

Approach

Initially it was considered that a magneto-optic sensor could be developed for an uncomplicated, noninvasive system. Such a noninvasive system would be capable of being installed on a power line without interrupting service and without dismantling any of the sensor optical path. Generally, optical fiber connectors are available but undesirable due to inherent coupling losses. In one case [2], such a noninvasive system has been documented, but most others are an invasive type requiring either optical connectors or service interruption [3],[4],[5]. The magneto-optic component of the noninvasive sensor consisted of only an optical fiber with one end mirrored and the other end attached to a light source and analysis equipment.

The invasive devices suggested an investigation of the rare-earth iron garnets, which exhibit very large Verdet constants in the range of 5-45 degrees of rotation per millimeter of path length at 1900 Oersteds and 20°C [6]. By using garnets, very accurate measurements could presumably be made with small sensors at low field intensities. In contrast, flint glass has a Verdet constant of 0.04 degree/mm, yet this is the material from which a working invasive sensor was built [4].

Possible configurations for a noninvasive sensor utilizing the iron garnets included the use of bulk crystals and thin films. One proposed bulk configuration involved building a device which

allowed the incident light to travel around one half of the conductor circumference and be mirrored back through the same path to provide an effective path of an entire trip around the conductor. Thus the noninvasive characteristics could be maintained and the output polarization would still be the same as the polarization achieved via a closed loop around the conductor. A second bulk material method would require that the garnet material be formed into a fiber which could then be used in the same manner as Rogers' device described previously. A thin film sensor could be essentially the same as the first bulk sensor with the exception that the thin film would reside on a substrate. A final configuration possibility would be to place a thin film and substrate against the conductor, perpendicular to the conductor magnetic field. The incident light would be introduced in such a manner as to reflect within the thin film in a zig-zag direction along the conductor. Thus, the light would have a large component of its path in the direction of the field and would experience a cumulative Faraday rotation while travelling through the film.

Unfortunately, the ferrimagnetic rare-earth iron garnets exhibit certain undesirable characteristics. Most important among these drawbacks is the temperature dependence of their Verdet constants [6]. Until suitable temperature compensation techniques are developed, the garnet-based sensors would be limited to a precision of only 5-10% over a 110°C temperature range [4],[6]. For metering purposes in the U.S., sensors are required to be precise to at least 0.1% or 0.3% depending upon classification.

Other drawbacks for the garnets include cost and availability. By the nature of their manufacture, the materials are expected to be much more expensive than flint glass or the common elements. Furthermore, at present the laboratories at Texas A&M would not be capable of growing the rare-earth iron garnet thin films without significant capital expenditures. Thus, it was concluded that another approach to developing a current sensor was needed.

The Electric Power Research Institute (EPRI) has confirmed that magneto-optic current sensors are not accurate enough, in general, to be used for monitoring power systems. EPRI did not, however, provide any new alternatives to the conventional transformer sensor. As stated previously, current transformer/-transducer systems are very accurate (some showing extremely high precision, 0.0001% in laboratory situations) in the field, but through extended usage their insulation breaks down and the multi-ton devices sometimes explode [7]. This type of failure is occurring with increasing frequency due to the growing demand on the national power grid and the concomitant higher load seen by each transformer.

A fiber optic current sensing system could provide complete insulation, due to the insulating properties of glass, and totally eliminate the possibility of explosive failure. EPRI recognized these facts in their report, but they do not support the continued investigation into such systems. EPRI has stated that eventually optical systems will be developed, and at such time the industry should consider a phase-out of existing transformer sensors. Until

the optical sensors do appear, however, EPRI has promulgated a generally negative view of magneto-optic current sensors without providing any leads to new breakthroughs in the sensor field.

One lead, which has presented itself as the most significant breakthrough of the preliminary research, is the use of a magnetostrictive material in a temperature compensating or self-compensating configuration. Such a device would involve the coupling of a magnetostrictive material to an optical temperature sensor. Thus, the device could measure both current, as an AC signal, and temperature, as an essentially DC signal. Magnetostriction, like the Faraday effect, is a phenomenon which has been known for many years. Magnetostriction has no rigorous physical explanation, rather, the equations describing it are heavily rooted in empirical measurements. Because of this lack of understanding, it has typically been viewed mainly as another magnetic curiosity. Unlike the Faraday effect, however, elements such as iron, nickel, and cobalt exhibit medium to high magnetostrictive tendencies relative to certain ferrites which also have very high magnetostriction constants but much more complex crystal structures [8]. In terms of laboratory complexity, the sputtering or evaporation of Fe, Ni, or Co onto an optical fiber is much easier than trying to grow crystals of cobalt-zinc-ferrites onto a fiber. The latter option is most likely impossible.

A fiber optic temperature sensor has been developed at Texas A&M involving the temperature modulation of the length of an optical resonant cavity [1]. In practice, a temperature sensor is

constructed by coating one end of a fiber with a thin layer of titanium oxide (TiO), which acts as a partial mirror. A second piece of fiber a few millimeters to a few centimeters in length is then fused to the mirrored end of the first fiber and another mirror layer of TiO is coated on the free end of the second fiber to make a resonant fiber cavity. The thickness of the TiO layers and the length of the cavity fiber are chosen for the light wavelength used and the temperature near which the sensor is intended to operate. Since the quartz (SiO_2) of the fiber has a known coefficient of thermal expansion, the temperature of the sensor is found by measuring the change in length of the cavity. A simple interferometer can measure this change with a submicron accuracy by monitoring the change in interference fringes between light waves incident upon the cavity and light waves returning from the cavity. This process results in very accurate temperature measurements.

To obtain current measurements from a temperature sensor, a suitable magnetostrictive material need only be clad to the fiber cavity. Then, as the magnetic field changes, the magnetostrictive material will stretch or shrink thereby causing the entire cavity length to be modulated. For a power system (50 or 60 Hz), the field-induced modulation will occur at 100 or 120 Hz, respectively, which is a much faster rate than the temperature-induced change. The signals can be filtered appropriately to determine temperature and field intensity. If, however, a constant DC magnetic field is present (due to direct current in the conductor), two sensors could

positioned so that one indicated a positive DC field and the other a negative DC field. In placing one parallel and the other antiparallel to the field, it should be possible to unambiguously determine all three quantities: AC field, DC field, and temperature.

Preliminary Results

Nickel was chosen as the testbed magnetostrictive material since it exhibits a polycrystalline magnetostriction constant

$$\bar{\lambda} = \frac{\Delta l}{l} = -32.94 \times 10^{-6}$$

which is a moderate value. Notably, the thermal expansion coefficient temperature dependence is still somewhat less ($\sim 0.4\,\bar{\lambda}$) than the magnetostriction constant magnitude over a wide temperature range (0°C-150°C) [8]. The deciding factor in choosing nickel, however, was that it is less expensive and easier to work with than the more highly magnetostrictive ferrites.

Once a suitable fiber cavity has been made, it must be clad with the nickel by electroplating to achieve the desired thickness. Since nickel will not plate directly to the SiO_2 fiber, a very thin (500Å) layer of titanium or chromium is sputtered onto the fiber to provide a conductive coating for electroplating and a strong interface between the fiber and the nickel layer. A cross-sectional schematic of the fiber and cladding is shown in Fig. 1. If chromium is used as an interface, its sputtering is immediately followed by a thin sputtering of nickel to prevent detrimental oxidation of the chromium in the atmosphere. Nickel is not sputtered directly onto the fiber because it would not bond as tightly to the SiO_2 as titanium or chromium would bond to both the nickel layer and the fiber. If this precautionary step were

eliminated, the nickel layer might separate from the fiber under high field intensities, thereby ruining the fiber.

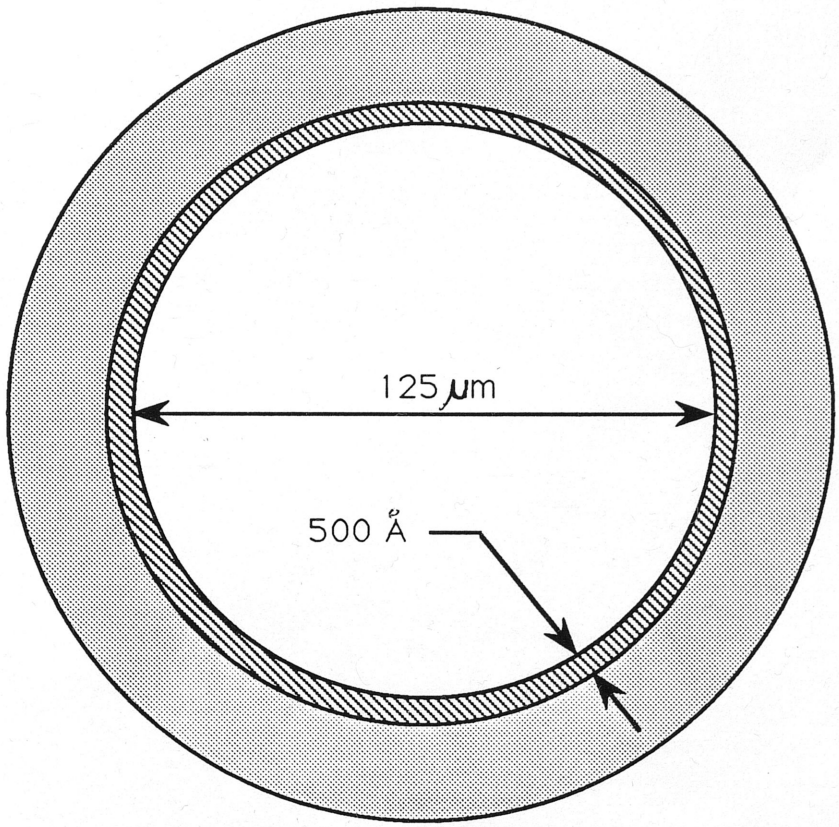

Figure 1. Cross Section of the Current Sensor Fiber. The hatched area is the Cr/Ni base and the shaded region is the electroplated Ni.

Using known physical constants for the elastic moduli of fused silica (SiO_2) fibers and elemental nickel, the thickness of the nickel layer required to achieve a certain change in cavity length is shown in Fig. 2. The deposition curves shown allow for consideration of initial cavity length, optical wavelength used, and required nickel thickness. These calculations were made for a fiber of circular cross-section with a diameter of 150 microns. The elastic effect of the titanium or chromium layer has been

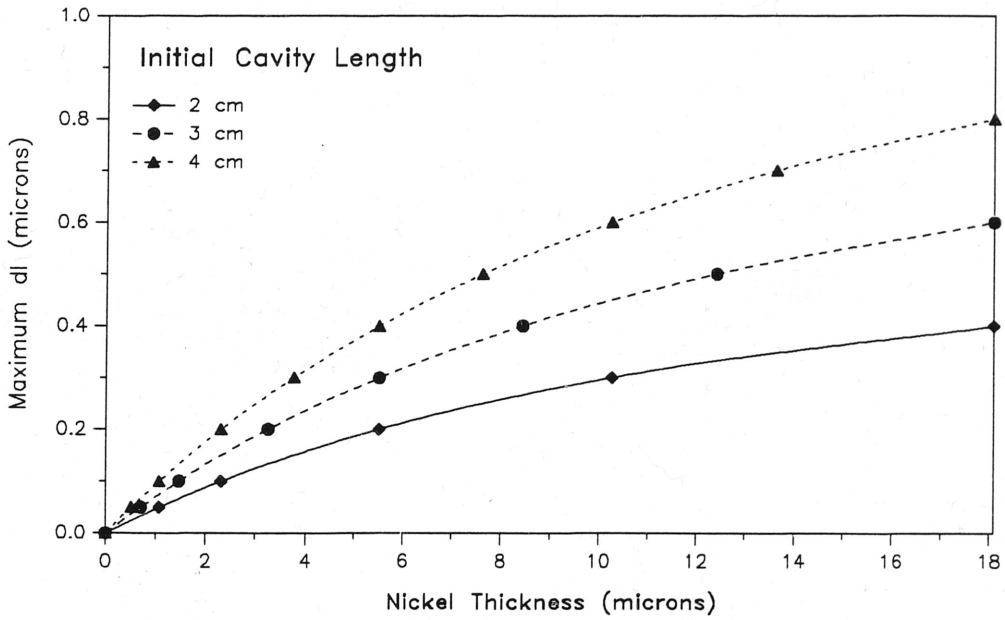

Figure 2. Calculated Maximum Magnetostriction vs. Nickel Thickness.

neglected due to its relative thinness. Since most optical fibers operate most efficiently at wavelengths around 1.2μm, and an interferometer will be unambiguous for changes in cavity length up to one quarter of a wavelength, the desired maximum change in cavity length is 0.3μm. Among the three initial cavity lengths presented in Fig. 2, the 4 cm cavity requires only ~3.8 μm of nickel, while the 3 cm and 2 cm cavities would need ~5.4 μm and ~10.3 μm, respectively, for the same response.

Part Two — Laboratory Research

While results of the preliminary research centered around applying nickel to a Fabry-Perot interferometer with high-reflectance mirrors, a much greater amount of time was spent in the laboratory on the more mundane aspect of process refinement. In particular, the electroplating procedures, well known to many electrochemists and professional electroplaters, required a great deal of preparation for application to fibers.

Initial practice involved learning to plate nickel onto simple objects such as small pieces of metal and gold-coated microscope slides. (The gold-coated slides were byproducts of gold evaporation and deposition runs for other researchers in the laboratory. As such, they were an economical use of a commodity which would otherwise have been lost.) Mostly, this stage of practice was necessary to learn the basics of electroplating. There were instances in which the polarity of the electrodes was reversed, or the current density was excessively high or low. Progress through this stage was very quick, however, and it only required a few more runs to determine the approximate characteristics of the plating solution being used, and what results could be expected for a range of operating conditions.

The general setup for electroplating consisted of a 1-liter straight-walled, battery-jar-style, beaker with a Teflon lid and Teflon-coated electrode holders; a platinum mesh electrode; a Hewlett-Packard or Kepco DC power supply; a Keithley Instruments

electrometer; a hot plate with magnetic stirring capabilities; and a thermometer. The beaker with a Teflon lid is a typical setup for electroplating since most work in the laboratory can easily fit into the beaker. The Teflon pieces were required to help prevent corrosion caused by the acidic plating solutions. Likewise, the platinum electrode served as a good all-purpose inert electrode. Platinum's low electronegativity relative to most other compounds has lead to it being called a 'noble metal', similar to the 'noble' or inert gases. In particular, it was found that metals accidently electroplated to the platinum, such as gold or nickel, could be easily removed via an acid etchant solution for the appropriate metal.

Both DC power supplies were capable of either voltage control or current control. Typically, they were used in the current-control mode since electroplating is dependent on current density rather than electrode potential difference. Electroplating current was estimated based on a recommended current density specific to the plating solution used and an estimate of the surface area of the piece being plated.

Just as the plating solution had recommended current densities, the hot plate and stirrer were necessary to maintain the apparatus at appropriate temperature and agitation levels. Operating temperature is quite specific and must be kept within a narrow range for optimum results. See Appendix A for more details.

The transition from plating flat surfaces like slides to cylindrical surfaces such as optical fibers required very few

changes in the equipment setup. The flat platinum mesh electrode was replaced with a 2.5 cm diameter cylindrical mesh fashioned specifically for plating fibers. Likewise, a cylindrical brass four-jawed fiber vise was obtained to make electrical contact to the surface of the fiber and to hold the fibers securely in place during plating. The vise and cylindrical electrode were constructed as a matching pair such that the vise was capable of being socketed into the electrode via a ceramic spacer ring. Thus, it was easily assured that the fibers could be placed within the geometric center of the electrode, maintaining a uniform plating ion concentration around the fiber over the length of the mesh electrode. The active region of the mesh electrode was only 5 cm long, but uniform plating was still achieved on fibers which extended beyond the electrode into the solution. The axial length of nickel plated to the fibers depended entirely on the length of the base coating of chromium and nickel which was electron-beam deposited onto the fiber. Typical e-beam deposition lengths ranging between 4 cm and 6 cm comprised the active plating region. By keeping only a minimum of the active region (0.25 cm to 0.5 cm) out of the plating bath, it was still possible to uniformly plate most of the submerged active region. The greatest irregularities, which were caused by fluctuating current density, occurred at the meniscus of the solution on the fiber.

The solution used for electroplating nickel was the commercial Watts bath made by the Transene Company, Inc. of Rowley, Massachusetts. Typical Watts bath solutions are composed of nickel

sulfate, nickel chloride, and boric acid, with proprietary buffers added for stability and ease of use [9]. Refer to Appendix B for the a list of the standard Watts bath compounds.

Another medium tested for nickel deposition was an ammoniacal autocatalytic, or 'electroless', solution. This mixture, also from Transene, was produced for applying nickel to semiconductor grade silicon. The solution was capable of depositing nickel without the use of an externally applied current, hence the name 'electroless'. It was found, however, that the electroless solution would neither deposit nickel to nickel-coated fibers nor to bare fibers. Upon determining that the electroless solution was essentially useless, attention promptly returned to electrolytic plating.

On the whole, the electroplating process was somewhat successful. A process for depositing under twenty microns of nickel was developed, but the coatings tended to be very fragile and could not withstand bending, especially for thicknesses greater than 10μm. Figure 3 is a photograph taken at 80× magnification depicting some of the problems experienced with plating thicker layers of nickel. Fig. 3 shows the nickel apparently erupting from the surface of the fiber. This damage was caused by current density fluctuations during plating. The current density was so high at the points of the rupture, that the metal formed blobs rather than a smooth layer around the fiber. Likewise, Fig. 4, which was taken at 100×, shows the brittle nature of the metallic coating. This fiber was damaged while being carried vertically in the laboratory. The fiber was bent at approximately 15° due to the

wind resistance of the fiber at a slow walking pace. It is suspected that the base coating of chromium and nickel were not properly bonded to the SiO_2 cladding of the fiber for both figures.

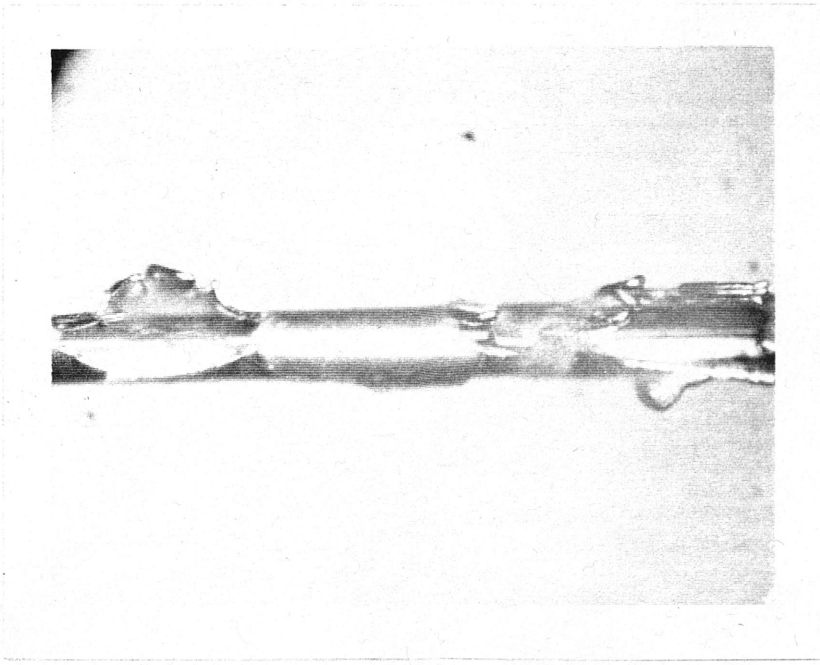

Figure 3. A failed Ni plating attempt. Note eruptions and peeling of the metal from the fiber wall. 80x.

These adhesion problems were quite daunting since it was shown early on that nickel could be successfully electroplated to the fibers at thicknesses of 2-3μm, but according to the preliminary calculations a much thicker layer would be necessary to achieve a desirable level of sensitivity. The key to solving the problem lay in a better process for attaching the nickel. In the two-step process of e-beam evaporation and electroplating, the initial stage of cleaning the fibers involved a physical stripping of the polymer buffer similar to removing insulation from a wire. This process is

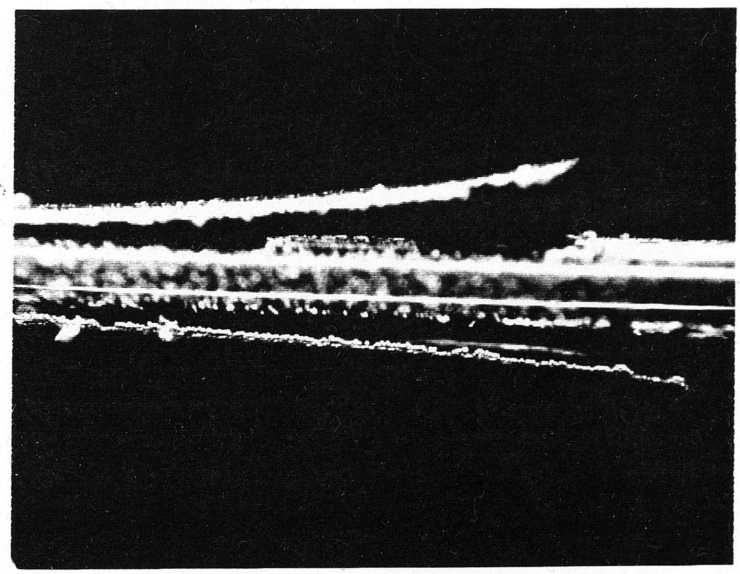

Figure 4. Another failed plating attempt. Note how the nickel cracked away from the fiber due to bending. 100×.

common among those who are interested only in the end of the fiber (e.g. for cleaving or mirroring the ends), but it is wholly unsuitable for preparing the sides to receive depositions. In the failures mentioned previously, it was suspected (but not directly confirmed) that the fibers had sustained damage to their cladding, still had polymer buffer residue clinging to their sides, or both.

In order to eliminate the likelihood of any buffer remaining on the fiber walls, a rigorous cleaning process used. The fibers were first treated with the solvent Dynasolve to remove all traces of polymer without physically scraping it off. Then, the fibers were rinsed with successive baths of acetone, isopropanol, and methanol, which form a standard cleansing sequence for optic and microelectronic device fabrication. Finally, rather than attempt

another e-beam deposition, a DC-sputter of nickel was performed.

The DC-sputter is possibly one of the simplest metal deposition machines. Argon gas is introduced into a high-vacuum chamber and ionized by a 4kV potential. A nickel source, or 'target' is placed at one electrode and the substrate being coated is placed at the other. Argon ions strike the nickel target with sufficient energy to dislocate nickel atoms, forming a gas of nickel and argon. The nickel atoms then coat whatever they contact. If the substrate (the fiber) is nearby, it will be coated with nickel. In the case of round objects such as fibers, DC-sputtering tends to cover more than just the upper projection, or top 180°, of the body. The metal atoms tend to flow around the sides of the body, usually coating at least 260° of its surface.

The decision to utilize a DC-sputter was based on its high rates of nickel deposition and the immediate availability of the machine in the lab. The DC-sputter was also expected to provide adequate adhesion, since concurrent research within the lab had found that several microns of titanium could be deposited successfully. The provisions for successful deposition, however, were that continuous deposition time be limited to 20 minutes with cooling periods of 10 to 20 minutes in between. These cool-down periods helped prevent the formation of cracks in the deposited material. Such cracks are known to adversely affect the adhesion of metals to nonmetallic substrates.

The total time required to deposit nickel on six fibers was less than 24 hours, which was an incredibly short turnaround time

that had not been enjoyed previously during the months of e-beam and electroplating trials. The fibers were soaked in Dynasolve overnight, and rinsed and loaded into the DC-sputter chamber the next morning. By afternoon, the chamber had been evacuated. The total deposition on-time was 57 minutes, which was divided into cycles of 20 minutes on and 10 minutes off. Initially, it was expected that 60 minutes of deposition would yield approximately one micron of nickel on only a portion of the surface of the fiber. Thus, it was expected that the fibers would need to be rotated and another run performed.

Surprisingly, the 57 minute deposition yielded approximately 2.5μm all the way around the fibers. This was a phenomenal success. The length of fiber coated varied between 20 cm and 25 cm, with approximately 15 cm of each fiber having the 2.5 μm layer. A tapering of nickel thickness toward the ends of the deposits was expected since the nature of the DC-sputter process is that the amount deposited is inversely proportional to the distance from the target to the substrate.

In terms of solving the adhesion problems previously experienced, the DC-sputter performed wonderfully. The fibers could be bent and handled without damage. But, there was still concern as to whether the thinner, longer coatings could be shown to be sensitive to magnetic fields that could be generated within the lab. Calculations had shown that a 1 μm thick, ~10 cm long layer of nickel should show detectable responses to magnetic fields in the range of 10-100 Oersteds. (In air, 1 Oersted corresponds to

1 Gauss, and 1 Gauss equals 0.1 millitesla.) Thus, it was wholly expected that encouraging results would be found.

Upon obtaining a successfully coated fiber, it was promptly installed in a two-armed Mach-Zehnder interferometer for initial testing. While the one-armed Fabry-Perot interferometer was the subject of preliminary interest, it was determined that the simpler Mach-Zehnder would be used. The Fabry-Perot would have provided many beneficial characteristics during the late stages of development and production of the sensor. These are, in particular, the ability to need only one fiber to obtain AC measurements and the potential ease with which the internally mirrored fiber could be coated with nickel.

As discussed in the preliminary research, a single fiber in the Fabry-Perot configuration could readily sense AC fields, but could not necessarily distinguish between DC magnetic fields and temperature-induced noise. The addition of a second reference interferometer would provide the extra information required to distinguish between signals. This is certainly a drawback, however, for someone wishing to measure AC and DC fields with only one interferometer.

The second benefit of the Fabry-Perot sensor deals with laboratory processes, which should be simplified as much as possible to improve product yield. By starting the nickel deposition phase with working Fabry-Perot interferometers, the overall sensor system is more quickly constructed. The Fabry-Perot is very delicate however, and the time-loss associated with the

accidental breakage of one of the interferometers is large.

Thus, the heightened possibility of breakage in lab, coupled with the high cost of obtaining optical equipment for the Fabry-Perot, forced the use of the simpler Mach-Zehnder interferometer. Whereas the Mach-Zehnder could use practically any laser diode as a light source, the Fabry-Perot required a very stable, high quality laser diode. During the construction of the Fabry-Perot, it is essentially referenced to itself via the use of a low noise, stable laser. The Mach-Zehnder avoids such problems because it has an external reference arm. Thus, the laser diode used was only a relatively cheap model manufactured primarily for use in the compact disc players. As a more concrete example of the tolerance of the Mach-Zehnder to nonideal circumstances, the laser operated at a wavelength of 0.85μm while the fibers were designed to be operated at the 1.3μm wavelength.

Construction of the Mach-Zehnder interferometer, performed by Dr. C.E. Lee, was not exceptionally difficult, but there were certain problems associated with fusion-arc splicing the nickel coated fibers to uncoated fibers. In one instance, the attempt was made to splice a heavily coated section of the sensor arm fiber to a normal fiber, but once the arc was struck an entire millimeter of nickel and fiber was evaporated, causing minor damage to the splicing machine. After a few more trials, an interferometer having a 15cm active (nickel coated) region on the sensing arm was completed.

The final phase of research involved the setup of a testbench

suitable for determining the characteristics of the Mach-Zehnder current sensor. This involved coaxing four major system components into useful operation. Along with the interferometer, the support and test equipment included a laser and its power supply, a photodetector and signal analyzer, and an electromagnet for producing magnetic test fields.

The electromagnet, with its field strength versus current graph shown in Fig. 5, was scavenged from a dismantled ion implanter that was being removed from the lab. A Variac variable autotransformer was used to power the magnet from the mains at 110 V, 60 Hz. Since the voltage was limited to 110 V for both practical and safety reasons, the highly inductive magnet allowed only 0.36 A to flow through it prior to implementing capacitive power factor correction. As can be seen from Fig. 5, the field induced by 0.36 A through the magnet was less than 80 Oersteds. By connecting a bank of parallel capacitors in series with the magnet, currents in excess of 1.4 A were achieved. The magnet's field strength due to 1.4 A is approximately 300 Oersteds.

The need for larger test fields was due to difficulties experienced by the lock-in amplifiers used for signal analysis. The UDT detector used for photoelectrical signal conversion introduced a significant amount of noise, such that the amplifiers were unable to lock in when operating at lower field strengths. Initially, this caused concern that the interferometer was not working properly. By increasing the magnetic field strengths, a marked increase in signal strength was observed, allowing the

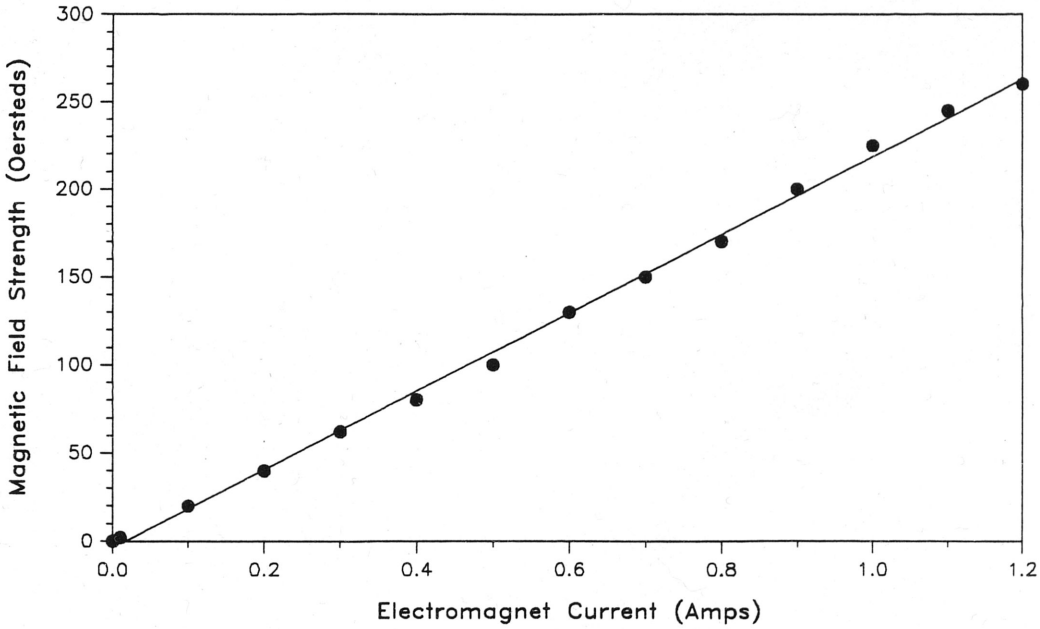

Figure 5. Electromagnet field strength vs. current characteristics.

amplifiers to lock in accurately. Figures 6, 7, and 8 provide a graphical depiction of the significance of power factor correction.

Figure 6 shows the baseline AC output of the UDT when connected directly to an oscilloscope. The laser was on, but the electromagnet current was off. Next, Fig. 7 shows the UDT output when the electromagnet current was only 0.36 A. Note that a 120 Hz signal is barely noticeable. When the current was increased to 1.0 A, however, the 120 Hz signal shown in Fig. 8 is readily detected.

The two lock-in amplifiers used were made by Princeton Applied Research (PAR) and Ithaco. The PAR machine was an older analog model which did not pick up the UDT signal well enough to stabilize on it. It is likely that the signal was somewhat unstable, as was experienced in working with the oscilloscope, thus causing the amplifier to have problems with locking in. By 'locking in', it is

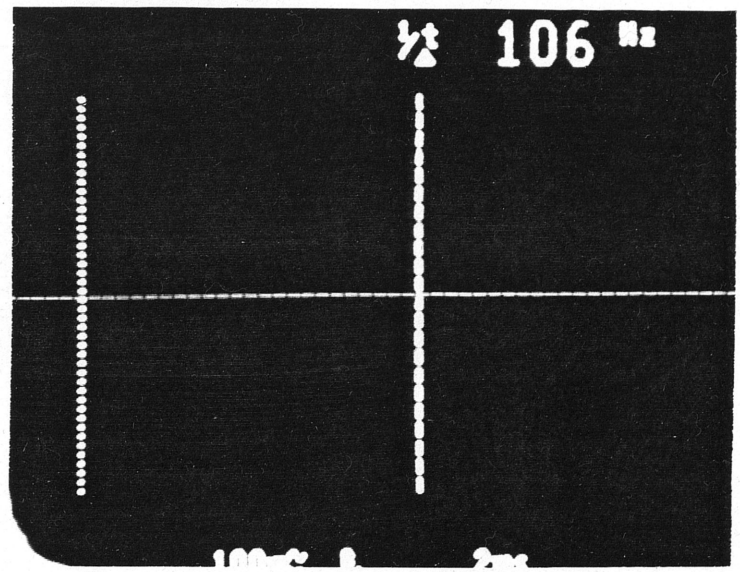

Figure 6. UDT photodetector output with electromagnet current off and laser on.

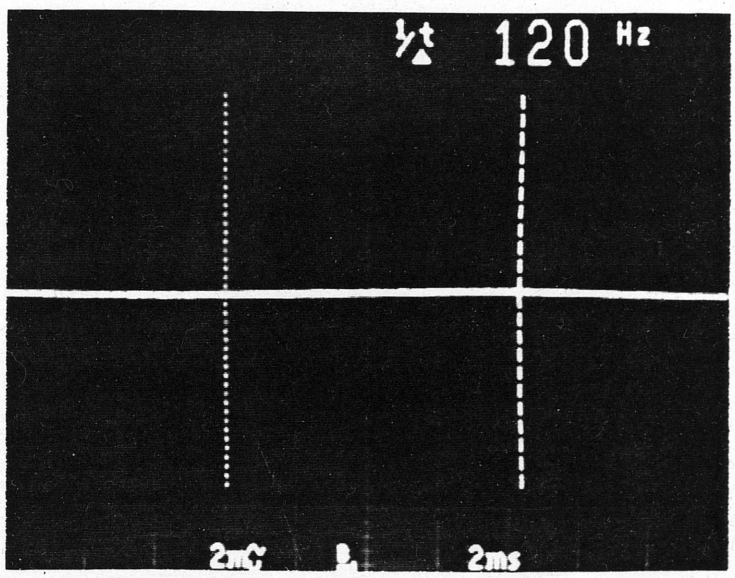

Figure 7. UDT output when electromagnet current is 0.36 A. A 120 Hz signal is barely detectable. Oscilloscope AC sensitivity is 2 mV per vertical division.

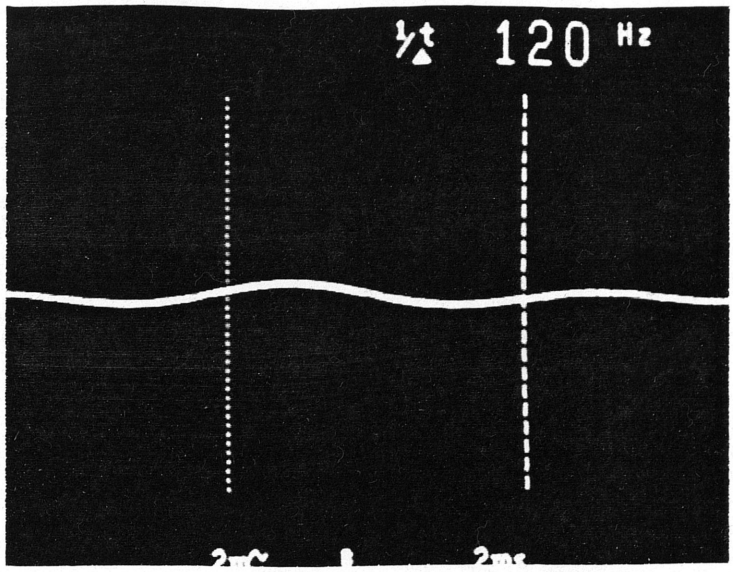

Figure 8. UDT output when electromagnet current is 1.0 A. Note the characteristic 120 Hz output signal. Oscilloscope AC sensitivity is 2 mV per vertical division.

meant that the machine can match a certain reference frequency with the same frequency in the input signal. The amplifiers are unable to lock in when either the magnitude of the externally applied reference is too small, or the applied signal is not stable relative to the internal reference.

The major problems experienced with the lock-in amplifiers were due to the instability and very small magnitude of the signal from the UDT. A workable solution was found by sending the signal through the Ithaco digital amplifier to a strip-chart recorder. The Ithaco amplifier was still unable to lock in via its internal reference oscillator, but the resultant output signal sent to the chart recorder was significant. The chart output consisted of a 0.2 Hz sinusoid with an amplitude proportional to the square of the

electromagnet current. The 0.2 Hz beat frequency was due to the amplifier's improperly calibrated internal oscillator. While the amplifier thought it was operating at 120 Hz, it was actually operating at 119.8 Hz, thus causing the low beat frequency.

Laboratory Results

Just as Figs. 7 and 8 show the output of the interferometer current sensor connected to an oscilloscope, Fig. 9 is a graph of the output of the lock-in amplifier (in millivolts) in relation to the square of the electromagnet current (in amps^2). The graph has two important characteristics, which are the existence of a sensitivity threshold and a quadratic nature with respect to magnetic field.

Magnetic theory predicts that the total magnetization of ferromagnetic materials, such as nickel, is proportional to the square of the applied external magnetic field if there is minimal internal magnetization. If the internal magnetization of the

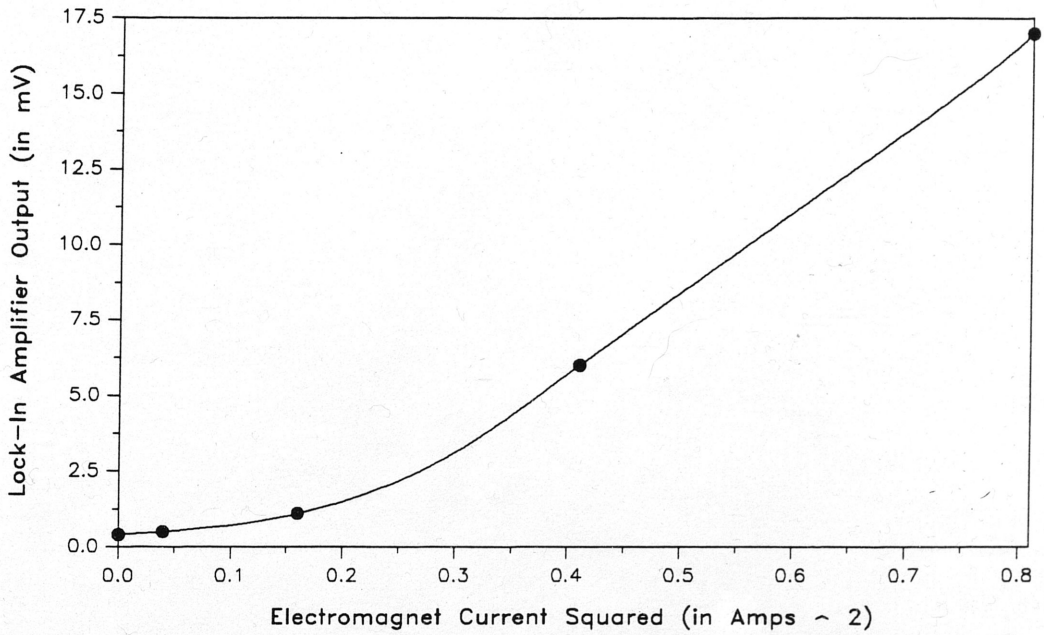

Figure 9. Initial sensor results. Lock-in amplifier output relative to electromagnet current squared. Note the threshold sensitivity corresponding to a magnetic field of 40 Oersteds.

material is sufficiently large (thousands of Oersteds), the total magnetization will appear linearly proportional in relation to smaller applied fields. Thus, in theory, the sensor could be linearly sensitive to AC fields if a large bias or dither field were applied, but such fields are impractical from an applications standpoint [10].

Even though the quadratic response is quite small and, of course, nonlinear, the interferometer is capable of detecting these minute changes of sensor arm length and conveying the information optically as a modulation of output power. When the level of output power decreases below a certain threshold the UDT and lock-in amplifier are unable to discriminate the signal from background noise. The threshold for the system under test is at approximately 0.04 A^2 (or 0.2 A electromagnet current) from Fig. 9, corresponding to about 40 Oersteds.

This threshold is not believed to be the absolute minimum sensitivity. It is, more likely, a rather high threshold caused by an accumulation of minor problems within the test setup. By properly providing an external reference for the lock-in amplifier and obtaining a less noisy UDT or replacing it with a more sensitive APD (avalanche photodetector), the effective sensitivity of the interferometric sensor would rise significantly. And, by increasing the length of the nickel coated 'active site' of the sensing arm, greater sensitivity will be achieved.

Conclusions

While it may appear that the research has taken a drastic change away from the originally proposed study of magneto-optics, the goal of optical current sensor proof-of-concept and development has been significantly advanced through the serendipitous realization that magnetostriction and temperature compensation can be directly coupled into a single device. There is still some concern that EPRI should take an active, positive, interest in magneto-optic current sensors, but to proceed with that very costly experimentation when a more promising, more unique, and less expensive possibility awaits virtually unexplored would be a questionable venture.

The current or magnetic field sensing capabilities of the magnetostrictive interferometer have been demonstrated. Granted, the device certainly is not ready for market, but it is ready for more in-depth research. The next logical phase of investigation would involve the complete characterization of the Mach-Zehnder configuration of the sensor prior to incorporating the concept in an internally-mirrored Fabry-Perot interferometer.

Conceivably, the sensor system could be miniaturized by using integrated circuit lock-in amplifiers, smaller photodetectors, and a dedicated laser power supply to achieve cigar-box geometries. Such a system, if accurate enough to meet the requisite industry standards, would be a vast improvement over present current sensing technology. Without doubt, however, there are still many obstacles to overcome prior to completion of the current sensor development.

References

[1] C.E. Lee, *Internal Mirror Technique For Fiber Optic Applications*. Dissertation. College Station, TX: Texas A&M University, 1988.

[2] A.J. Rogers, "A vibration-insensitive optical-fibre current sensor," *Proc. of SPIE*, vol. 630, pp. 180-186, 1986.

[3] B.T. Neyer, J. Chang, and L.E. Ruggles, "Calibrated Faraday current and magnetic field sensor," *Proc. of SPIE*, vol. 566, pp. 201-205, 1985.

[4] Y. Kuroda *et al.*, "Field test of fiber-optic voltage and current sensors applied to gas insulated substations," *Proc. of SPIE*, vol. 586, pp. 30-37, 1985.

[5] M. Kanoi, G. Takahashi, and T. Sato, "Optical voltage and current measuring system for electric power systems," *IEEE Trans. Power Del.*, vol. PWRD-1, no. 1, pp. 91-97, Jan. 1986.

[6] R.C. Booth and E.A.D. White, "Magneto-optic properties of rare earth iron garnet crystals in the wavelength range 1.1-1.7μm and their use in device fabrication," *J. Phys. D: Appl. Phys.*, vol. 17, pp. 579-587, 1984.

[7] D.L. Hillhouse, *Optical Power Line Voltage and Current Measurement Systems*. Palo Alto, CA: Electric Power Research Institute, Sept. 1987. EPRI EL-5431.

[8] S. Chikazumi and S.H. Charap, *Physics of Magnetism*. Huntington, NY: Krieger, 1978.

[9] F.A. Lowenheim, *Electroplating*. New York: McGraw-Hill, 1978.

[10] A.D. Kersey and A. Dandridge, "Applications of fiber-optic sensors," *IEEE Trans. Components, Hybrids and Mfg. Tech.*, vol. 13, no. 1, pp. 137-143, Mar. 1990.

Appendix A

These are tables of data taken while electroplating nickel on optical fibers. A base coat of chromium and nickel had been previously applied via electron beam deposition to facilitate electroplating metal to the quartz fibers.

The information is for three runs on two fibers, on which a few microns of nickel were successfully coated before the process failed. In both cases, the length of nickel-coated fiber in the solution was 45-55 mm. Note that these were very long, slow depositions, planned in an effort to minimize irregularities in the plated nickel. Trials 1 and 2 were on the same fiber.

Trial 1.

Stage	Current (mA)	Start Temp (°C)	Stop Temp (°C)	Time (min.)
1	0.10	51	49	15
2	0.15	49	49	15
3	0.30	49	59	31
4	0.60	59	58	29

Trial 2.

Stage	Current (mA)	Start Temp (°C)	Stop Temp (°C)	Time (min.)
1	0.20	53	54	30
2	0.60	54	52	75
3	0.20	52	54	15

Trial 3.

Stage	Current (mA)	Start Temp (°C)	Stop Temp (°C)	Time (min.)
1	0.10	55	53	15
2	0.15	53	52	15
3	0.30	52	59	30
4	0.60	59	62	120
5	0.20	62	56	15

Appendix B

The typical Watts nickel electroplating solution and suggested operating characteristics are given below [9].

	Range		Usual	
	g/ℓ	molarity	g/ℓ	molarity
$NiSO_4 \cdot 6H_2O$	225-375	0.86-1.43	330	1.25
$NiCl_2 \cdot 6H_2O$	30-60	0.13-0.25	45	0.19
Total Ni	58-100	1-1.68	85	1.44
H_3BO_3	30-40	0.5-0.65	37	0.60
Anti-pit (30% H_2O_2)			0.5 mℓ/ℓ per day	
Sodium Lauryl Sulfate			?	
Temperature °C	45-65		60	
pH	1.5-4.5		3-4	
Current density (A/m^2)	250-1000		500	